

# Light Higgsino Dark Matter

Manuel Drees<sup>1</sup>, Mihoko M. Nojiri<sup>2</sup>, D.P. Roy<sup>3</sup> and Youichi Yamada<sup>4</sup>

<sup>1</sup>*APCTP, College of Natural Sciences, Seoul National University, Seoul 151-742, Korea*

<sup>2</sup>*KEK Theory Group, Oho-ho 1-1, Tsukuba, Ibaraki, 305 Japan*

<sup>3</sup>*Tata Institute of Fundamental Research, Homi Bhabha Road, Mumbai 400005, India*

<sup>4</sup>*Department of Physics, Tohoku University, Sendai, 980-77, Japan*

## Abstract

We re-investigate the question whether a light higgsino-like neutralino is a viable Dark Matter candidate. To this end we compute the dominant one-loop corrections to the masses of the higgsino-like states in the minimal Supersymmetric Standard Model (MSSM), due to loops involving heavy quarks and their superpartners. We also calculate analogous corrections to the couplings of higgsino-like neutralinos to  $Z$  and Higgs bosons. In the region of parameter space leading to high higgsino purity of the lightest neutralino, these corrections can change the expected relic density by up to a factor of five in either direction. We conclude that for favorable choices of soft supersymmetry breaking parameters, a state with more than 99% higgsino purity could indeed form all cold Dark Matter in the Universe. In some cases these corrections can also increase the expected cross section for LSP scattering off spinless nuclei by up to two orders of magnitude, or reduce it to zero.

# 1) Introduction

It has been known for more than ten years that the lightest supersymmetric particle (LSP) can be a good candidate for the missing “Dark Matter” (DM) in the Universe [1, 2]. In models with conserved “R parity” the LSP is absolutely stable. Searches for exotic isotopes [3] then imply that it must be electrically and color neutral. Within the particle content of the Minimal Supersymmetric Standard Model (MSSM) this leaves us with two kinds of candidates, the lightest sneutrino  $\tilde{\nu}$  and the lightest neutralino  $\tilde{\chi}_1^0$ . A combination of “new physics” searches at the CERN  $e^+e^-$  collider LEP and direct DM search experiments excludes the sneutrino as viable DM candidate [2]. This leaves us with the lightest neutralino.

In general the lightest neutralino  $\tilde{\chi}_1^0$  is a superposition of the  $U(1)_Y$  gaugino  $\tilde{B}$  (“bino”), the neutral  $SU(2)$  gaugino  $\tilde{W}_3$ , and the two higgsinos  $\tilde{h}_1^0$  and  $\tilde{h}_2^0$  (with  $Y_{\tilde{h}_1} = -Y_{\tilde{h}_2} = -1/2$ ). A gaugino-dominated state (photino or bino) has the right relic density [4, 5] to provide the missing Dark Matter if  $m_{\tilde{l}_R}^4/m_{\tilde{\chi}_1^0}^2 \simeq (200 \text{ GeV})^2$ , which points towards the same range of superparticle masses favored by naturalness arguments; here  $\tilde{l}_R$  stands for  $SU(2)$  singlet sleptons, whose exchange dominates the annihilation of bino-like neutralinos since they have the largest hypercharge. Originally it was thought [4] that a sufficiently pure higgsino-state would also give an interesting relic density, if it is lighter than the  $W$  boson so that  $\tilde{\chi}_1^0\tilde{\chi}_1^0 \rightarrow W^+W^-$  is kinematically suppressed. The reason is that the coupling of a pair of higgsino-like LSPs to a  $Z$  boson becomes very small if the gaugino masses are much larger than the higgsino mass parameter. However, Mizuta and Yamaguchi [6] later realized that the standard estimate [2] for the LSP density is not reliable in this case. The reason is that there are actually three higgsino-like states, two neutralinos and one chargino. The mass splitting between these states becomes very small as the gaugino masses become large. In such a situation one has to include “co-annihilation” between the LSP and these only slightly heavier states [7]. Note that the  $Z\tilde{\chi}_1^0\tilde{\chi}_2^0$  and  $W\tilde{\chi}_1^0\tilde{\chi}_1^\pm$  couplings are large if the LSP is dominantly a higgsino. Co-annihilation therefore greatly reduces the estimate for the relic density of a higgsino-like LSP [5, 6].

So far the discussion was based essentially on tree-level results (although QCD corrections were taken into account in the leading logarithmic approximation by using “running” quark masses and couplings [5]). More recently, complete one-loop electroweak radiative corrections to the masses of the neutralinos and charginos have become available [8]. Using these general results, Giudice and Pomarol very recently pointed out [9] that loop corrections can quite significantly change the mass splitting between the three higgsino-like states, the dominant contribution coming from loops involving heavy quarks ( $t, b$ ) and their superpartners. This is of some relevance for superparticle searches at LEP, since the heavier higgsino-like states will be quite difficult to detect experimentally if their decays only deposit a few GeV of visible energy in the detector.\*

Here we point out that these radiative corrections can also change the estimate of the LSP relic density quite dramatically, since the co-annihilation rate depends exponentially on the mass splitting between the higgsino-like states. Radiative corrections also change the decomposition of the LSP, which alters its couplings to gauge and Higgs bosons. These couplings are further modified by explicit vertex corrections. We present a full calculation of these three-point function corrections due to Yukawa interactions. Their effect on the relic density is relatively modest, but for negative sign of the higgsino mass parameter they can

---

\*In this case one can still search for events where the heavier higgsinos are produced in association with a hard, isolated photon. This signal should be viable [10] even in the limit of almost perfect mass degeneracy, but the cross section is considerably smaller than for the simple pair production process.

change the cross section for LSP scattering off spinless nuclei by two orders of magnitude.

The remainder of this article is organized as follows. In Sec. 2 we describe the formalism, including one-loop corrections to the masses and relevant couplings of higgsinos. In Sec. 3 we present numerical results for the LSP relic density and its detection rate in a  $^{76}\text{Ge}$  detector. Our estimate of the relic density includes a careful treatment of  $s$ -channel poles [7], as well as “sub-threshold annihilation” [7] into  $W$  and Higgs boson pairs. Our estimate of the LSP detection rate includes the full set of contributions discussed in ref.[11]. In Sec. 4 we summarize our results and present some conclusions. Finally, in the Appendix we list expressions for three-point functions in the kinematical configurations of interest to us.

## 2) Formalism

In this section we describe the calculation of the one-loop corrections to the mass of the higgsino-like states, as well as to the couplings of the LSP to  $Z$  and Higgs bosons. We focus here on corrections from Yukawa couplings, which give the potentially largest contributions to the mass splittings [9] and couplings of interest to us.

### 2a) Corrections to the Masses

The corrections to the mass splittings can be understood as corrections to the chargino and neutralino mass matrices. Including one-loop corrections to the higgsino masses, these matrices can be written as

$$\mathcal{M}_{\pm} = \begin{pmatrix} M_2 & \sqrt{2}M_W \sin\beta \\ \sqrt{2}M_W \cos\beta & \mu + \delta_C \end{pmatrix} \quad (1a)$$

$$\mathcal{M}_0 = \begin{pmatrix} M_1 & 0 & -M_Z \cos\beta \sin\theta_W & M_Z \sin\beta \sin\theta_W \\ 0 & M_2 & M_Z \cos\beta \cos\theta_W & -M_Z \sin\beta \cos\theta_W \\ -M_Z \cos\beta \sin\theta_W & M_Z \cos\beta \cos\theta_W & \delta_{33} & -\mu - \delta_{34} \\ M_Z \sin\beta \sin\theta_W & -M_Z \sin\beta \cos\theta_W & -\mu - \delta_{34} & \delta_{44} \end{pmatrix} \quad (1b)$$

Here  $M_1$  and  $M_2$  are the supersymmetry breaking masses of the  $U(1)_Y$  and  $SU(2)$  gauginos, respectively,  $\mu$  is the higgsino mass parameter, and  $\tan\beta = \langle H_2^0 \rangle / \langle H_1^0 \rangle$  is the ratio of vacuum expectation values of the two neutral Higgs fields of the MSSM [12, 13].

Note that we are only interested in states that are (almost) pure higgsinos. We do therefore not include contributions that are suppressed by both loop factors and small higgsino-gaugino mixing angles. This is why we only included corrections to the higgsino entries of the mass matrices. Further, since we focus on corrections due to Yukawa couplings, we only need to consider quark-squark loops. Their contributions are given by [8]:

$$\begin{aligned} \delta_C = & -\frac{3}{32\pi^2} \Re \left\{ h_b h_t \sin(2\theta_{\tilde{b}}) m_t \left[ B_0(Q, t, \tilde{b}_1) - B_0(Q, t, \tilde{b}_2) \right] \right. \\ & + h_b h_t \sin(2\theta_{\tilde{t}}) m_b \left[ B_0(Q, b, \tilde{t}_1) - B_0(Q, b, \tilde{t}_2) \right] \\ & + \mu \left[ \left( h_b^2 \sin^2 \theta_{\tilde{b}} + h_t^2 \cos^2 \theta_{\tilde{b}} \right) B_1(Q, t, \tilde{b}_1) + \left( h_b^2 \cos^2 \theta_{\tilde{b}} + h_t^2 \sin^2 \theta_{\tilde{b}} \right) B_1(Q, t, \tilde{b}_2) \right. \\ & \left. \left. + \left( h_t^2 \sin^2 \theta_{\tilde{t}} + h_b^2 \cos^2 \theta_{\tilde{t}} \right) B_1(Q, b, \tilde{t}_1) + \left( h_t^2 \cos^2 \theta_{\tilde{t}} + h_b^2 \sin^2 \theta_{\tilde{t}} \right) B_1(Q, b, \tilde{t}_2) \right] \right\}; \end{aligned} \quad (2a)$$

$$\delta_{34} = -\frac{3\mu}{32\pi^2} \Re \left\{ h_t^2 \left[ B_1(Q, t, \tilde{t}_1) + B_1(Q, t, \tilde{t}_2) \right] + h_b^2 \left[ B_1(Q, b, \tilde{b}_1) + B_1(Q, b, \tilde{b}_2) \right] \right\}; \quad (2b)$$

$$\delta_{33} = -\frac{3}{16\pi^2} h_b^2 m_b \sin(2\theta_{\tilde{b}}) \Re \left\{ B_0(Q, b, \tilde{b}_1) - B_0(Q, b, \tilde{b}_2) \right\}; \quad (2c)$$

$$\delta_{44} = -\frac{3}{16\pi^2} h_t^2 m_t \sin(2\theta_{\tilde{t}}) \Re \left\{ B_0(Q, t, \tilde{t}_1) - B_0(Q, t, \tilde{t}_2) \right\}. \quad (2d)$$

Here  $B_0$  and  $B_1$  are two-point functions, for which we use the conventions of refs.[8]. Their first argument is the external momentum scale  $Q$ , and the second and third arguments are a quark and squark mass, for which we wrote the symbol of the corresponding fields in order to avoid double subscripts. The squark masses are eigenvalues of the  $\tilde{t}$  and  $\tilde{b}$  mass matrices [14], which we write in the basis  $(\tilde{q}_L, \tilde{q}_R)$  following the notation of ref.[15]:

$$\mathcal{M}_{\tilde{t}}^2 = \begin{pmatrix} m_t^2 + m_{\tilde{t}_L}^2 + \left(\frac{1}{2} - \frac{2}{3} \sin^2 \theta_W\right) \cos(2\beta) M_Z^2 & -m_t (A_t + \mu \cot \beta) \\ -m_t (A_t + \mu \cot \beta) & m_t^2 + m_{\tilde{t}_R}^2 + \frac{2}{3} \sin^2 \theta_W \cos(2\beta) M_Z^2 \end{pmatrix} \quad (3a)$$

$$\mathcal{M}_{\tilde{b}}^2 = \begin{pmatrix} m_b^2 + m_{\tilde{t}_L}^2 - \left(\frac{1}{2} - \frac{1}{3} \sin^2 \theta_W\right) \cos(2\beta) M_Z^2 & -m_b (A_b + \mu \tan \beta) \\ -m_b (A_b + \mu \tan \beta) & m_b^2 + m_{\tilde{b}_R}^2 - \frac{1}{3} \sin^2 \theta_W \cos(2\beta) M_Z^2 \end{pmatrix} \quad (3b)$$

Note that  $SU(2)$  invariance implies that the soft breaking terms appearing in the (1,1) entries of the mass matrices (3a) and (3b) are equal. The lighter eigenstates are defined as  $\tilde{q}_1 = \tilde{q}_L \cos \theta_{\tilde{q}} + \tilde{q}_R \sin \theta_{\tilde{q}}$ . Finally,  $h_b$  and  $h_t$  in eqs.(2) are the Yukawa couplings of the  $b$  and  $t$  quarks:

$$h_b = \frac{gm_b}{\sqrt{2}M_W \cos \beta}; \quad h_t = \frac{gm_t}{\sqrt{2}M_W \sin \beta}, \quad (4)$$

where  $g$  is the  $SU(2)$  gauge coupling, and the quark masses are to be taken at scale  $Q$ .

As written, the corrections  $\delta_C$  and  $\delta_{34}$  are divergent. The fact that the divergence is the same for these two quantities provides a nontrivial check of our calculation. This divergence has to be absorbed by renormalizing the higgsino mass parameter  $\mu$ . We have used the  $\overline{\text{DR}}$  renormalization scheme, with renormalization scale taken equal to the external momentum scale  $Q$ . For consistency, the tree-level parameter  $\mu$  in eqs.(1) then has to be interpreted as running mass taken at the same scale  $Q$ . In principle one has to diagonalize the matrices of eqs.(1) at different  $Q = m_{\tilde{\chi}_i^0}$  or  $Q = m_{\tilde{\chi}_i^\pm}$  in order to compute the physical (on-shell) neutralino and chargino masses. However, since the  $Q$ -dependence of the corrections is quite weak, for our purposes it is sufficient to compute the mass matrices at fixed  $Q = |\mu|$ .

For our later discussion it is convenient to have approximate analytical expressions for the masses of the higgsino-like states as well as for the LSP eigenvector. In the for us relevant limit  $M_1, M_2 \gg |\mu|$  the mass of the lighter chargino is approximately

$$m_{\tilde{\chi}_1^\pm} \simeq |\mu_C| \left[ 1 - \frac{M_W^2 \sin(2\beta)}{\mu_C M_2} \right] + \mathcal{O}(M_2^{-2}), \quad (5)$$

where  $\mu_C = \mu + \delta_C$ ; see eq.(1a).

In the same limit the two lightest neutralinos are approximately equal to the symmetric and anti-symmetric combination of the two higgsino current eigenstates  $\tilde{h}_1^0$  and  $\tilde{h}_2^0$ . Including terms up to first order in small quantities, their eigenvectors are given by: <sup>†</sup>

$$N_{\tilde{h}_S^0} \simeq \left( \epsilon_1^{(S)}, \epsilon_2^{(S)}, \frac{1}{\sqrt{2}} + \epsilon_3, \frac{1}{\sqrt{2}} - \epsilon_3 \right); \quad (6a)$$

---

<sup>†</sup>In our convention the neutralino eigenvectors are real, and we keep the signs of the eigenvalues.

$$N_{\tilde{h}_A^0} \simeq \left( \epsilon_1^{(A)}, \epsilon_2^{(A)}, \frac{1}{\sqrt{2}} - \epsilon_3, -\frac{1}{\sqrt{2}} - \epsilon_3 \right), \quad (6b)$$

with

$$\epsilon_1^{(S,A)} = \frac{M_Z \sin\theta_W}{M_1} \cdot \frac{\cos\beta \mp \sin\beta}{\sqrt{2}}; \quad (7a)$$

$$\epsilon_2^{(S,A)} = -\frac{M_Z \cos\theta_W}{M_2} \cdot \frac{\cos\beta \mp \sin\beta}{\sqrt{2}}; \quad (7b)$$

$$\begin{aligned} \epsilon_3 &= \frac{M_Z^2 \cos(2\beta)}{4\sqrt{2}\mu_N} \left( \frac{\sin^2\theta_W}{M_1} + \frac{\cos^2\theta_W}{M_2} \right) + \frac{\delta_{44} - \delta_{33}}{4\sqrt{2}\mu_N} \\ &= \frac{\sqrt{2}M_W^2 \cos(2\beta)}{5\mu_N M_2} + \frac{\delta_{44} - \delta_{33}}{4\sqrt{2}\mu_N}, \end{aligned} \quad (7c)$$

with  $\mu_N = \mu + \delta_{34}$ . The upper (lower) sign in eqs.(7a,b) holds for the symmetric (anti-symmetric) higgsino state. The second equality in eq.(7c) is valid only if one assumes the usual “unification condition”

$$M_1 = \frac{5}{3} \tan^2\theta_W M_2 \simeq 0.5M_2. \quad (8)$$

The masses of the higgsino-like eigenstates are given by

$$\begin{aligned} m_{\tilde{h}_{S,A}^0} &\simeq \mp\mu_N - \frac{M_Z^2}{2} (1 \mp \sin(2\beta)) \left( \frac{\sin^2\theta_W}{M_1} + \frac{\cos^2\theta_W}{M_2} \right) + \frac{1}{2} (\delta_{33} + \delta_{44}) \\ &\simeq \mp\mu_N - \frac{4M_W^2}{5M_2} (1 \mp \sin(2\beta)) + \frac{1}{2} (\delta_{33} + \delta_{44}), \end{aligned} \quad (9)$$

where we have kept the signs of the eigenvalues, and the second equality again assumes eq.(8).

If the second term in eq.(9) is larger than the loop corrections given by the third term, which is generally the case for  $M_2 \leq 1$  TeV, the LSP will be the symmetric (anti-symmetric) higgsino state if  $\mu$  is negative (positive). For small and moderate values of  $\tan\beta$  this distinction is quite important, since the anti-symmetric higgsino-like state has larger gaugino components, see eqs.(7a,b). Moreover, the mass splitting between the higgsino-like states also depends on the sign of  $\mu$ . Assuming for simplicity eq.(8) to hold, one has [9]

$$\left| m_{\tilde{\chi}_2^0} - m_{\tilde{\chi}_1^0} \right| \simeq \left| \frac{8M_W^2}{5M_2} - \delta_{33} - \delta_{44} \right|; \quad (10a)$$

$$m_{\tilde{\chi}_1^\pm} - \left| m_{\tilde{\chi}_1^0} \right| \simeq \frac{M_W^2}{5M_2} [4 - \text{sign}(\mu) \sin(2\beta)] - \frac{1}{2} (\delta_{33} + \delta_{44}) + \delta_C - \delta_{34}. \quad (10b)$$

Note that the one-loop corrections increase (decrease) the mass splittings if  $\delta_{33} + \delta_{44}$  is negative (positive). As already pointed out in ref.[9], this correction can be quite significant. In contrast, we found that the last term in eq.(10b),  $\delta_C - \delta_{34}$ , is negligible in all cases.

## 2b) Corrections to the Couplings

At tree level the  $Z\tilde{\chi}_1^0\tilde{\chi}_1^0$  coupling is proportional to the tree-level contribution to  $\epsilon_3$ ; this coupling largely determines the annihilation rate of higgsino-like LSPs. However, at one-loop level one has to include the explicit vertex correction diagrams of Figs. 1a,b as well

as the (off–diagonal) wave function renormalization diagram of Fig. 1c. We compute these corrections in the limit where the lighter neutralinos are exact higgsino; at the end we include mixing by simply multiplying the correction with the relevant higgsino component of the eigenstates. This procedure greatly simplifies the calculation. In this limit the only non–vanishing  $Z$ –neutralino coupling is the off–diagonal  $Z\tilde{\chi}_1^0\tilde{\chi}_2^0$  coupling, so we do not need to include any diagonal wave function renormalization diagrams. Note also that there is no vertex counter–term, since Yukawa couplings do not renormalize gauge couplings at one–loop level. Our procedure will give reliable results as long as the gaugino components  $\epsilon_1, \epsilon_2$  in eqs.(6) are small. When these components become sizable or even dominant, our procedure may no longer give an accurate estimate of the loop corrections; however, in this case the loop corrections are in any case much smaller than the tree–level contributions to the mass splittings and couplings of interest to us, so that we again only make a small error.

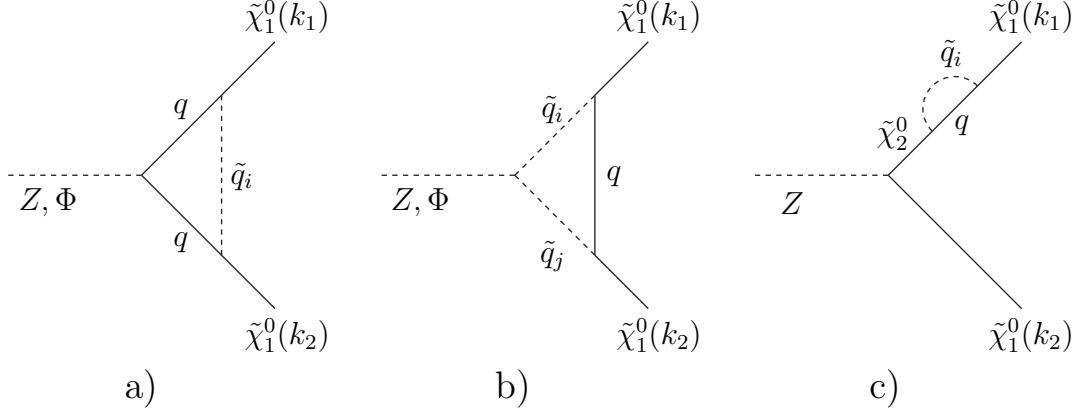


**Fig. 1:** Quark–squark loop corrections to the coupling of a pair of LSPs to a  $Z$  or Higgs boson. The LSP momenta  $k_1$  and  $k_2$  point towards the vertex. Note that both senses of the “Dirac arrow” (flow of fermion number) have to be added, since the LSP is a Majorana fermion. There is also a diagram of type c) with a quark–squark bubble on the other neutralino line. There are two squark mass eigenstate with a given flavor.

The diagrams of Fig. 1 can be described by the following effective  $Z\tilde{\chi}_1^0\tilde{\chi}_1^0$  vertex:

$$\delta\Gamma_{Z\tilde{\chi}\tilde{\chi}}^\mu = -i\frac{3g}{8\pi^2\cos\theta_W} \left[ \left( N_{13}^2 h_b^2 \delta_a^{(b)} + N_{14}^2 h_t^2 \delta_a^{(t)} \right) \gamma^\mu \gamma_5 + \left( N_{13}^2 h_b^2 \delta_p^{(b)} + N_{14}^2 h_t^2 \delta_p^{(t)} \right) (k_1^\mu + k_2^\mu) \gamma_5 \right], \quad (11)$$

where  $N_{13}$  and  $N_{14}$  are the third and fourth component of the LSP eigenvector, and  $k_1$  and  $k_2$  are the momenta of the two neutralinos. We use the tensor decomposition of the three–point function as given in ref.[16]; this form is convenient for the case of two equal external masses. The coefficients  $\delta_{a,p}$  of eq.(11) can then be written as:

$$\delta_a^{(q)} = [c_{a,q} + c_{v,q} \cos(2\theta_{\tilde{q}})] \left[ \left( m_{\tilde{\chi}_1^0}^2 - k_1 \cdot k_2 \right) C_2^+(\tilde{q}_1) + \left( m_{\tilde{\chi}_1^0}^2 + k_1 \cdot k_2 \right) C_2^-(\tilde{q}_1) \right. \\ \left. + C_2^0(\tilde{q}_1) + m_{\tilde{\chi}_1^0}^2 \left( \frac{1}{2} C_0(\tilde{q}_1) - 2C_1^+(\tilde{q}_1) \right) + \frac{1}{2} m_q^2 C_0(\tilde{q}_2) \right]$$

$$\begin{aligned}
& + [c_{a,q} - c_{v,q} \cos(2\theta_{\tilde{q}})] \left[ \left( m_{\tilde{\chi}_1^0}^2 - k_1 \cdot k_2 \right) C_2^+(\tilde{q}_2) + \left( m_{\tilde{\chi}_1^0}^2 + k_1 \cdot k_2 \right) C_2^-(\tilde{q}_2) \right. \\
& \quad \left. + C_2^0(\tilde{q}_2) + m_{\tilde{\chi}_1^0}^2 \left( \frac{1}{2} C_0(\tilde{q}_2) - 2C_1^+(\tilde{q}_2) \right) + \frac{1}{2} m_q^2 C_0(\tilde{q}_1) \right] \\
& - \frac{1}{2} c_{a,q} + m_q m_{\tilde{\chi}_1^0} c_{a,q} \sin(2\theta_{\tilde{q}}) \left[ C_0(\tilde{q}_1) - 2C_1^+(\tilde{q}_1) - C_0(\tilde{q}_2) + 2C_1^+(\tilde{q}_2) \right] \\
& - \cos(2\theta_{\tilde{q}}) \left[ \left( -I_{3,q} \cos^2\theta_{\tilde{q}} + e_q \sin^2\theta_W \right) C_2^0(\tilde{q}_1, \tilde{q}_1) + \left( I_{3,q} \sin^2\theta_{\tilde{q}} - e_q \sin^2\theta_W \right) C_2^0(\tilde{q}_2, \tilde{q}_2) \right] \\
& + I_q \sin^2(2\theta_{\tilde{q}}) C_2^0(\tilde{q}_1, \tilde{q}_2) - \frac{I_q}{2} [B_1(\tilde{q}_1) + B_1(\tilde{q}_2)] \\
& + \frac{m_q I_q}{2m_{\tilde{\chi}_1^0}} \sin(2\theta_{\tilde{q}}) [B_0(\tilde{q}_2) - B_0(\tilde{q}_1)] \tag{12a}
\end{aligned}$$

$$\begin{aligned}
\delta_p^{(q)} & = m_{\tilde{\chi}_1^0} \left\{ [c_{a,q} + c_{v,q} \cos(2\theta_{\tilde{q}})] [2C_2^-(\tilde{q}_1) - C_1^+(\tilde{q}_1)] + [c_{a,q} - c_{v,q} \cos(2\theta_{\tilde{q}})] [2C_2^-(\tilde{q}_2) - C_1^+(\tilde{q}_2)] \right. \\
& \quad + 2 \cos(2\theta_{\tilde{q}}) \left[ \left( -I_{3,q} \cos^2\theta_{\tilde{q}} + e_q \sin^2\theta_W \right) C_2^-(\tilde{q}_1, \tilde{q}_1) + \left( I_{3,q} \sin^2\theta_{\tilde{q}} - e_q \sin^2\theta_W \right) C_2^-(\tilde{q}_2, \tilde{q}_2) \right] \\
& \quad \left. - 2I_q \sin^2(2\theta_{\tilde{q}}) C_2^-(\tilde{q}_1, \tilde{q}_2) \right\} \\
& + m_q \sin(2\theta_{\tilde{q}}) \left\{ -c_{a,q} [C_1^+(\tilde{q}_1) - C_1^+(\tilde{q}_2)] - I_{3,q} C_1^-(\tilde{q}_1, \tilde{q}_2) \right\}. \tag{12b}
\end{aligned}$$

Here we have used the shorthand notation  $C_k(\tilde{q}_i) = C_k(s, m_{\tilde{\chi}_1^0}^2, m_q, m_{\tilde{q}_i})$ ,  $C_k(\tilde{q}_i, \tilde{q}_j) = C_k(s, m_{\tilde{\chi}_1^0}^2, m_{\tilde{q}_i}, m_{\tilde{q}_j}, m_q)$  and  $B_k(\tilde{q}_i) = B_k(m_{\tilde{\chi}_1^0}^2, m_q, m_{\tilde{q}_i})$ . Recall that we use the  $B_1$  function of refs.[8], which differs from that of ref.[16] by an overall sign. Finally, the couplings in eqs.(12) are given by

$$c_{a,q} = \frac{1}{2} I_{3,q}; \quad c_{v,q} = -\frac{1}{2} I_{3,q} + e_q \sin^2\theta_W, \tag{13}$$

where  $I_{3,q} = \pm 1/2$  and  $e_q$  are the weak isospin and charge of quark  $q$ , respectively.

We note that one obtains a finite result only after summing over all three classes of diagrams and both squark eigenstates. Similarly, decoupling of degenerate heavy squarks ( $m_{\tilde{q}_1} \simeq m_{\tilde{q}_2} \rightarrow \infty$ ) only holds after summation over all three diagrams and both squark eigenstates. However, the very last contribution to  $\delta_a^{(q)}$ , eq.(12a), is by itself finite and shows the proper decoupling behaviour. In fact, it closely resembles the corrections  $\delta_{33}$  and  $\delta_{44}$  of eqs.(2c,d). Indeed, these two terms come from the same two-point function diagrams, see Fig. 1c. We can therefore include these terms either explicitly in  $\delta_a^{(q)}$ , or via the mass matrix corrections  $\delta_{33}$ ,  $\delta_{44}$ , where they change the quantity  $\epsilon_3$  given in eq.(7c); recall that this quantity determines the ‘‘tree-level’’  $Z\tilde{\chi}_1^0\tilde{\chi}_1^0$  vertex [12]:

$$\begin{aligned}
\Gamma_{Z\tilde{\chi}\tilde{\chi}}^{\mu, \text{tree}} & = i \frac{g}{2 \cos\theta_W} \gamma^\mu \gamma_5 (N_{13}^2 - N_{14}^2) \\
& \simeq \pm i \frac{g}{\cos\theta_W} \sqrt{2} \epsilon_3 \gamma^\mu \gamma_5, \tag{14}
\end{aligned}$$

where the (upper) lower sign is for the symmetric (anti-symmetric) higgsino-state, i.e. for negative (positive)  $\mu$ . Together with eq.(7c) this sign ensures that the sign of the correction to the  $Z\tilde{\chi}_1^0\tilde{\chi}_1^0$  coupling is independent of the sign of  $\mu$ . This can also be seen from the last contribution to  $\delta_a^{(q)}$ , of course, keeping in mind that the LSP mass is always positive, independent of the sign of  $\mu$ , see eq.(9). We find that this term usually gives the dominant contribution to  $\delta_a^{(q)}$ ; moreover, the  $\delta_p^{(q)}$  are usually quite small. One can therefore get a

rough estimate of the size of the loop contributions from the diagrams of Figs. 1 by simply diagonalizing the mass matrix (1b), including the corrections  $\delta_{33}$  and  $\delta_{44}$ , and using the “tree-level” vertex of eq.(14). Of course, one must not include this correction both in the mass matrix and in  $\delta_a^{(q)}$ .

We also computed one-loop corrections to the LSP coupling to the neutral Higgs bosons of the MSSM. These couplings are not so important for the estimate of the relic density, unless  $2m_{\tilde{\chi}_1^0}$  happens to be very close to or slightly lower than the mass of one of these Higgs bosons. However, the exchange of the neutral scalar Higgs bosons often gives the dominant contribution [17, 11] to elastic LSP–nucleus scattering. One therefore has to know these couplings quite accurately in order to make a reliable estimate of the event rate in various experiments that search for relic neutralinos. This is true both for direct detection experiments, which search for the recoil of nuclei struck by ambient LSPs, and for indirect detection experiments that search for neutrinos produced by LSP annihilation in the center of the Earth or Sun [18, 2]; the detection rate of the indirect search experiments is proportional to the rate with which ambient neutralinos are captured by the Earth or Sun, which in turn is proportional to the LSP scattering cross section off ordinary matter.

At tree-level a pure higgsino state has *no* couplings to Higgs bosons; these couplings originate from the Higgs–higgsino–gaugino interactions in the supersymmetric Lagrangian. This also implies that the wave function renormalization diagram of Fig. 1c does not contribute here.<sup>‡</sup> We therefore only have to evaluate the explicit vertex corrections of Figs. 1a,b.

Their contribution can be described by the effective vertices

$$i\delta\Gamma_{\phi\tilde{\chi}\tilde{\chi}} = -i\frac{3}{16\pi^2} \left( h_b^2 N_{13}^2 \delta_\phi^{(b)} + h_t^2 N_{14}^2 \delta_\phi^{(t)} \right); \quad (15a)$$

$$i\delta\Gamma_{A\tilde{\chi}\tilde{\chi}} = -\frac{3}{16\pi^2} \gamma_5 \left( h_b^2 N_{13}^2 \delta_A^{(b)} + h_t^2 N_{14}^2 \delta_A^{(t)} \right), \quad (15b)$$

where  $\phi$  stands for the light neutral scalar  $h^0$  or the heavy neutral scalar  $H^0$  and  $A$  is the pseudoscalar Higgs boson. The coefficients in eqs.(15) can be written as

$$\begin{aligned} \delta_\phi^{(q)} &= \frac{h_q r_\phi^{(q)}}{\sqrt{2}} \left\{ \sin(2\theta_{\tilde{q}}) \left[ \left( m_{\tilde{q}_1}^2 + m_q^2 + m_{\tilde{\chi}_1^0}^2 \right) C_0(\tilde{q}_1) - 4m_{\tilde{\chi}_1^0}^2 C_1^+(\tilde{q}_1) \right. \right. \\ &\quad \left. \left. - \left( m_{\tilde{q}_2}^2 + m_q^2 + m_{\tilde{\chi}_1^0}^2 \right) C_0(\tilde{q}_2) + 4m_{\tilde{\chi}_1^0}^2 C_1^+(\tilde{q}_2) \right] \right. \\ &\quad \left. + 2m_{\tilde{\chi}_1^0} m_q \left[ C_0(\tilde{q}_1) + C_0(\tilde{q}_2) - 2C_1^+(\tilde{q}_1) - 2C_1^+(\tilde{q}_2) \right] \right\} \\ &+ c_{\tilde{q},11}^{(\phi)} \left[ m_q \sin(2\theta_{\tilde{q}}) C_0(\tilde{q}_1, \tilde{q}_1) + 2m_{\tilde{\chi}_1^0} C_1^+(\tilde{q}_1, \tilde{q}_1) \right] \\ &+ c_{\tilde{q},22}^{(\phi)} \left[ -m_q \sin(2\theta_{\tilde{q}}) C_0(\tilde{q}_2, \tilde{q}_2) + 2m_{\tilde{\chi}_1^0} C_1^+(\tilde{q}_2, \tilde{q}_2) \right] + 2c_{\tilde{q},12}^{(\phi)} m_q \cos(2\theta_{\tilde{q}}) C_0(\tilde{q}_1, \tilde{q}_2); \quad (16a) \\ \delta_A^{(q)} &= \frac{h_q r_A^{(q)}}{\sqrt{2}} \left\{ \sin(2\theta_{\tilde{q}}) \left[ \left( m_q^2 + m_{\tilde{\chi}_1^0}^2 - m_{\tilde{q}_1}^2 \right) C_0(\tilde{q}_1) - \left( m_q^2 + m_{\tilde{\chi}_1^0}^2 - m_{\tilde{q}_2}^2 \right) C_0(\tilde{q}_2) \right] \right\} \end{aligned}$$

---

<sup>‡</sup>There are wave function renormalization diagrams where an external higgsino is converted into a gaugino, which then couples to the Higgs boson and the second higgsino. This gives contributions of order  $\frac{3}{16\pi^2} g^2 h_t m_t / M_2$ , which can be interpreted as  $\mathcal{O}(h_t^2)$  corrections to the tree-level coupling, which is of order  $gM_W/M_2$ . However, unlike our corrections  $\delta_{33}$  and  $\delta_{44}$  this only corrects an entry in the neutralino mass matrix that is already nonzero at tree-level, and will therefore change the LSP couplings to Higgs bosons by at most a few percent. In our case these corrections are further suppressed since we are interested in a higgsino-like LSP, which (for  $\tan\beta \neq 1$ ) implies  $M_1, M_2 \gg |\mu|$ ; diagrams with internal gaugino lines are then suppressed by the large gaugino masses.



$$\begin{aligned}
& + 2m_{\tilde{\chi}_1^0} m_q [C_0(\tilde{q}_1) + C_0(\tilde{q}_2)] \} \\
& + 2c_{\tilde{q},12}^{(A)} [m_q C_0(\tilde{q}_1, \tilde{q}_2) + 2m_{\tilde{\chi}_1^0} \sin(2\theta_{\tilde{q}}) C_1^-(\tilde{q}_1, \tilde{q}_2)]. \tag{16b}
\end{aligned}$$

Here we have used the same notation for the arguments of the  $C$  functions as in eqs.(12). The coefficients  $r_\phi^{(q)}$  and  $r_A^{(q)}$  describe the Higgs couplings to quarks; they are given by [13]:

$$\begin{aligned}
r_{H^0}^{(t)} &= -\frac{\sin\alpha}{\sin\beta}; & r_{h^0}^{(t)} &= -\frac{\cos\alpha}{\sin\beta}; & r_A^{(t)} &= -\cot\beta; \\
r_{H^0}^{(b)} &= -\frac{\cos\alpha}{\cos\beta}; & r_{h^0}^{(b)} &= \frac{\sin\alpha}{\cos\beta}; & r_A^{(b)} &= -\tan\beta, \tag{17}
\end{aligned}$$

where  $\alpha$  is the mixing angle of the neutral scalar Higgs bosons [13]. Finally, the coefficients  $c_{\tilde{q},ij}^{(\phi)}$  and  $c_{\tilde{q},12}^{(A)}$  describe the couplings of one Higgs boson to a pair of squarks; they are given by [19]

$$\begin{aligned}
c_{\tilde{q},11}^{(H^0)} &= -\frac{gM_Z \cos(\alpha + \beta)}{\cos\theta_W} [I_{3,q} \cos^2\theta_{\tilde{q}} - e_q \sin^2\theta_W \cos(2\theta_{\tilde{q}})] + \frac{gm_q^2}{M_W} r_{H^0}^{(q)} \\
& - \frac{h_q \sin(2\theta_{\tilde{q}})}{\sqrt{2}} (r_{H^0}^{(q)} A_q + r_{H^0}^{\prime(q)} \mu); \tag{18a}
\end{aligned}$$

$$\begin{aligned}
c_{\tilde{q},12}^{(H^0)} &= -\frac{gM_Z \cos(\alpha + \beta)}{\cos\theta_W} \sin(2\theta_{\tilde{q}}) \left[ e_q \sin^2\theta_W - \frac{I_{3,q}}{2} \right] \\
& - \frac{h_q \cos(2\theta_{\tilde{q}})}{\sqrt{2}} (r_{H^0}^{(q)} A_q + r_{H^0}^{\prime(q)} \mu); \tag{18b}
\end{aligned}$$

$$\begin{aligned}
c_{\tilde{q},11}^{(h^0)} &= \frac{gM_Z \sin(\alpha + \beta)}{\cos\theta_W} [I_{3,q} \cos^2\theta_{\tilde{q}} - e_q \sin^2\theta_W \cos(2\theta_{\tilde{q}})] + \frac{gm_q^2}{M_W} r_{h^0}^{(q)} \\
& - \frac{h_q \sin(2\theta_{\tilde{q}})}{\sqrt{2}} (r_{h^0}^{(q)} A_q + r_{h^0}^{\prime(q)} \mu); \tag{18c}
\end{aligned}$$

$$c_{\tilde{q},12}^{(h^0)} = \frac{gM_Z \sin(\alpha + \beta)}{\cos\theta_W} \sin(2\theta_{\tilde{q}}) \left[ e_q \sin^2\theta_W - \frac{I_{3,q}}{2} \right] - \frac{h_q \cos(2\theta_{\tilde{q}})}{\sqrt{2}} (r_{h^0}^{(q)} A_q + r_{h^0}^{\prime(q)} \mu); \tag{18d}$$

$$c_{\tilde{q},22}^{(\phi)} = c_{\tilde{q},11}^{(\phi)} (\cos\theta_{\tilde{q}} \rightarrow \sin\theta_{\tilde{q}}, \sin\theta_{\tilde{q}} \rightarrow -\cos\theta_{\tilde{q}}); \tag{18e}$$

$$c_{\tilde{q},12}^{(A)} = \frac{h_q}{\sqrt{2}} (r_A^{(q)} A_q + \mu) \times \begin{pmatrix} \sin\beta \text{ for } u \\ \cos\beta \text{ for } d \end{pmatrix}. \tag{18f}$$

Where

$$\begin{aligned}
r_{H^0}^{\prime(t)} &= -\frac{\cos\alpha}{\sin\beta}; & r_{h^0}^{\prime(t)} &= \frac{\sin\alpha}{\sin\beta}; \\
r_{H^0}^{\prime(b)} &= -\frac{\sin\alpha}{\cos\beta}; & r_{h^0}^{\prime(b)} &= -\frac{\cos\alpha}{\cos\beta}. \tag{19}
\end{aligned}$$

The  $A_q$  also appear in the squark mass matrices of eqs.(3), and  $I_{3,q}$  and  $e_q$  again refer to the weak isospin and charge of quark  $q$ . Finally, the Yukawa couplings  $h_q$  have been defined in eq.(4).

Note that the pseudoscalar Higgs boson has no couplings to two equal squark eigenstates [13].

We note that in this case the diagrams of the type shown in Fig. 1a are finite by themselves once one has summed over both squark eigenstates, and the diagrams of Fig. 1b are separately finite for each combination of squarks in the loop. Notice also that this last class of diagrams is proportional to the Higgs–squark–squark couplings, which receive contributions from the  $A_q$  parameters; these couplings can become very large [19].

As noted earlier, we use the  $C$  functions of ref.[16]. However, there is a technical complication. When estimating the LSP relic density we need to evaluate these functions at  $s = 4m_{\tilde{\chi}_1^0}^2$ , whereas LSP–nucleus scattering cross sections probe these functions at  $s \simeq 0$ . The expressions for the higher  $C$  functions given in Appendix C of ref.[16] contain apparent divergencies in *both* these limits. We stress that the loop functions themselves remain well behaved as  $s \rightarrow 4m_{\tilde{\chi}_1^0}^2$  or  $s \rightarrow 0$ ; the apparent divergencies in the expressions of ref.[16] therefore all cancel. In fact, even the standard expression for the scalar three–point function  $C_0$  contains apparent divergencies in the kinematical configurations of interest to us. In the case of  $C_0$  the necessary cancellation between different terms can still be accomplished numerically by slightly increasing or reducing  $s$ . However, for the higher  $C$  functions these cancellations become quite delicate. We therefore re–evaluated the relevant Feynman integrals for the two cases of interest to us. In both limiting situations the  $C$  functions can be expressed as combinations of two–point ( $B$ ) functions; all coefficients are now finite. The relevant expressions are collected in the Appendix.

### 3) Results

We are now in a position to present some numerical results. We focus on light higgsino–like states,  $m_{\tilde{\chi}_1^0} < M_W$ , since heavier LSPs have very large annihilation cross sections into  $W$  and  $Z$  pairs [20, 5]. A heavy higgsino therefore only makes a good cold Dark Matter (CDM) candidate if its mass exceeds 0.5 TeV. This is already uncomfortably heavy for “weak scale” supersymmetry; for example, assuming gaugino mass unification, the gluino mass has to be larger than 3 TeV in such scenarios. In fact, the annihilation cross section into  $W^+W^-$  final states is so large that it can be relevant even if the LSP mass is a little below  $M_W$ . Such “sub–threshold annihilation” can occur since at freeze–out the LSPs still have significant thermal energy. We include this effect for  $W^+W^-$  and also  $h^0h^0$  pairs in our estimate of the LSP relic density, using the formalism developed in ref.[7]. We also use a careful treatment of  $s$ –channel poles ( $Z$  and Higgs exchange diagrams); as pointed out in ref.[7], the standard expansion in the LSP velocity [1] breaks down in the vicinity of such poles. We use the numerical method developed in ref.[21].

In order to illustrate the effects of the loop corrections on the LSP couplings to Higgs bosons, we also present results for the LSP counting rate in an isotopically pure  $^{76}\text{Ge}$  detector, assuming a fixed local LSP mass density of 0.3 GeV/cm<sup>3</sup> [22] and a velocity dispersion of 320 km/sec. Nuclear effects are described by a Gaussian form factor, with a nuclear radius of 4.1 fm [23]. Of course, we could just as well have used any other spinless isotope. The scattering rate due to spin–dependent interactions is affected by the loop corrections to the  $Z\tilde{\chi}_1^0\tilde{\chi}_1^0$  coupling, but this correction is usually somewhat smaller than that to the LSP–Higgs couplings. Note that the total scattering cross–section off heavy nuclei is usually dominated by the spin–independent contribution even if the nucleus in question does have non–vanishing spin [24].

Since we are interested in scenarios with rather light LSP, we have to be careful not to

violate any experimental bounds. The most relevant constraints on the parameters appearing in the tree-level neutralino mass matrix comes from chargino searches at LEP [25]. Unfortunately these bounds are not entirely straightforward to interpret in our case, since the standard set of experimental cuts used to suppress SM backgrounds becomes quite inefficient in scenarios with small  $\Delta m_{\tilde{\chi}} \equiv m_{\tilde{\chi}_1^\pm} - m_{\tilde{\chi}_1^0}$ . Note also that the cross section for the production of higgsino-like charginos is smaller than for gaugino-like states. We interpret the LEP bounds as requiring

$$m_{\tilde{\chi}_1^\pm} \geq \begin{cases} 75 \text{ GeV}, & \Delta m_{\tilde{\chi}} \geq 10 \text{ GeV} \\ 45 \text{ GeV}, & \Delta m_{\tilde{\chi}} < 10 \text{ GeV} \end{cases} \quad (20)$$

The second bound comes from the measurement of the total width of the  $Z$  boson [27], and thus holds for any value of  $\Delta m_{\tilde{\chi}}$ . We are aware that this parametrization of the LEP search constraints is only a crude approximation, but it should be sufficient to illustrate the effects of the loop corrections.

We have seen in the previous section that these corrections depend on the details of the stop and sbottom mass matrices. In particular, the corrections  $\delta_{33}$  and  $\delta_{44}$  to the neutralino mass matrix are proportional to  $\sin(2\theta_{\tilde{q}})$ , see eqs.(2c,d); these corrections also vanish in the limit of equal masses for squarks of a given flavor. The combination of these two properties means that the corrections depend sensitively on the size of the off-diagonal entries of the squark mass matrices (3). Moreover, the potentially largest correction to the LSP-Higgs coupling, coming from the diagram of Fig. 1b, directly depends on the  $A$ -parameters appearing in the squark mass matrices. Third generation squarks also contribute to other loop processes. This imposes some constraints even on combinations of parameters where all squark mass eigenstates lie well above the direct experimental search limits [26, 27].

In ref.[9] the  $\tilde{t} - \tilde{b}$  loop contribution to the electroweak  $\rho$  parameter was emphasized. However, given that a “new physics” contribution  $\delta\rho \simeq 3 \cdot 10^{-3}$  is not excluded by present data [27], we find that other loop corrections lead to stronger constraints. In particular, loop corrections to the mass of the light neutral Higgs scalar  $h^0$  turn negative when  $A_t$  becomes too large [28]. One important constraint therefore comes from searches for the MSSM Higgs bosons at LEP [27].

The constraints we have discussed so far do not depend on the masses of the other squarks, and are therefore quite model-independent. If we make the additional simplifying assumption that all explicitly supersymmetry breaking diagonal squark masses ( $m_{\tilde{t}_L}$ ,  $m_{\tilde{t}_R}$  and  $m_{\tilde{b}_R}$  in eqs.(3), and analogous quantities for the first and second generation squarks) are equal at the weak scale, we find that the strongest constraint on the parameters of the stop mass matrix comes from the recent CLEO measurement [29] of the branching ratio for inclusive  $b \rightarrow s\gamma$  decays:

$$1 \cdot 10^{-4} \leq B(b \rightarrow s\gamma) \leq 4 \cdot 10^{-4}. \quad (21)$$

Since we are studying scenarios with rather light charginos, chargino-stop contributions to this partial width can be quite large [30]; they can be of either sign, depending on the signs of  $\mu$  and  $A_t$ . However, the resulting constraint is more model-dependent: If one allows some non-universality of soft-breaking squark masses, one also gets contributions from gluino-squark and neutralino-squark loops [30], the size of which depends strongly on the details of the entire three generation squark mass matrices. For definiteness we will stick to a scenario with exactly universal soft breaking squark masses, and with  $A_t = A_b \equiv A$ , with the understanding that the constraints that result from imposing the bounds (21) can be relaxed in slightly more general models without significantly changing the loop corrections to the masses and couplings

of higgsino-like states.

In Fig. 2 we show the dependence of various quantities relevant to our subsequent analysis, normalized such that they can be plotted to a common scale. We fixed  $M_2 = 350$  GeV and  $\mu = -70$  GeV, which means that the LSP is a more than 99% pure higgsino; we define the higgsino fraction as  $1 - \text{gaugino fraction} = 1 - (\epsilon_1^2 + \epsilon_2^2)$ , see eqs.(6). We chose  $\tan\beta = 1.5$  so that the top Yukawa coupling is close to its upper bound, if one requires it to remain perturbatively small all the way to the GUT scale; on the other hand,  $b-\tilde{b}$  loops are essentially negligible for such a small value of  $\tan\beta$ . We took a very large mass (1.5 TeV) for the pseudoscalar Higgs boson, since this maximizes  $m_{h^0}$ , and hence minimizes the impact of the LEP Higgs search bounds. This also means that charged Higgs boson loop contributions to the  $b \rightarrow s\gamma$  partial width are negligible. Our choice of 430 GeV for the common soft breaking squark mass is again motivated by our desire to maximize the size of the loop effects, given the experimental constraints discussed above. Increasing  $m_{\tilde{q}}$  for fixed  $A/m_{\tilde{q}}$  would reduce the ratio of physical stop masses, which leads to reduced  $t - \tilde{t}$  loop corrections. On the other hand, we cannot increase  $A/m_{\tilde{q}}$  beyond the limits shown in Fig. 2 without violating some experimental bound. Finally, here and in the subsequent figures we assume gaugino mass unification, eq.(8).

The curves in Fig. 2 terminate at values of  $A$  where  $m_{h^0}$  falls below the LEP bound of about 62 GeV; note that  $h^0$  is essentially indistinguishable from the single Higgs boson of the SM if  $m_A^2 \gg M_Z^2$ . The two dotted curves show a “high” and “low” theoretical estimate for  $B(b \rightarrow s\gamma)$ , scaled up by a factor  $10^4$ . Our estimates are based on a leading order QCD analysis [30], which has substantial scale uncertainties [31]; the band in Fig. 2 corresponds to varying the renormalization scale between 2.5 and 10 GeV, and also includes uncertainties from CKM matrix elements etc.<sup>§</sup> Notice that the “low estimate” can be zero. This happens if the contribution from sparticle loops is larger than that from the standard  $t - W$  loops and has opposite sign, reversing the sign of the complete matrix element at scale  $M_W$  or  $m_t$ . Renormalization group effects give another contribution from tree-level  $W$  exchange due to operator mixing; this contribution is not sensitive to any “new physics”. In the SM this term has the same sign as the loop matrix element at scale  $M_W$ , leading to a large QCD enhancement factor, but in the MSSM these two contributions can cancel. For fixed renormalization scale this cancellation only happens at specific points of SUSY parameter space, but perfect cancellation becomes possible for an entire range of parameters if the renormalization scale is allowed to vary.

We note that for the given sign of  $\mu$ , the branching ratio for inclusive  $b \rightarrow s\gamma$  decays tends to be below (above) the SM prediction if  $A$  is negative (positive). In order to be conservative, we only exclude combinations of parameters where the “high” theoretical estimate is below the lower bound, or the “low” estimate is above the upper bound, given in (21). For the parameters of Fig. 2 this translates into the constraint  $-2.7 \leq A/m_{\tilde{q}} \leq 2.65$ , which is only slightly stronger than that resulting from Higgs searches at LEP. Within this region,  $\delta\rho_{\tilde{t}\tilde{b}} \leq 2.2 \cdot 10^{-3}$ .

The solid curve in Fig. 2 shows  $\Delta m_{\tilde{\chi}}$  (divided by 5 GeV to fit the scale). The tree-level prediction for this quantity for the given choice of  $M_2$ ,  $\mu$  and  $\tan\beta$ , 14.5 GeV, is very close to the loop-corrected value for  $A = 0$ . We see that the corrections can either increase or decrease the chargino-LSP mass splitting by about 4 GeV before one gets into conflict with the constraint (21). In this case the loop corrections therefore only amount to at most 30%;

---

<sup>§</sup>Very recently an almost-complete next-to-leading order calculation of  $B(b \rightarrow s\gamma)$  in the framework of the MSSM has appeared [32]; their result falls within our band.

however, we will see below that this suffices to change the prediction for the LSP relic density quite dramatically.

Finally, the long and short dashed curves in Fig. 2 show the (re-scaled) couplings of the LSP to  $Z$  and  $h^0$  bosons, respectively;  $g_{Z\tilde{\chi}_1^0\tilde{\chi}_1^0}$  is defined as the axial vector coupling at  $s = 4m_{\tilde{\chi}_1^0}^2$ , while  $g_{h\tilde{\chi}_1^0\tilde{\chi}_1^0}$  is defined at  $s = 0$ . As in case of  $\Delta m_{\tilde{\chi}}$ , the tree-level predictions for these quantities are very close to the loop-corrected values at  $A = 0$ . We see that the relative variation in LSP- $Z$  coupling is larger than that in  $\Delta m_{\tilde{\chi}}$ , when  $A$  is varied over its allowed range. Note also the positive correlation between these two quantities, which reinforces the correlation between small  $\Delta m_{\tilde{\chi}}$  and small  $g_{Z\tilde{\chi}_1^0\tilde{\chi}_1^0}$  that holds for higgsino-like LSPs at tree-level, see eqs.(7c) and (10b). A similar correlation also holds for the loop-corrected coupling of the LSP to the light scalar Higgs boson, as shown by the short dashed curve. However, in this case the tree-level prediction is very small,  $g_{h\tilde{\chi}_1^0\tilde{\chi}_1^0} \simeq 7.6 \cdot 10^{-3}$ . This can be understood from eqs.(7a,b) and the general expression for this coupling given in ref.[13]:

$$\begin{aligned} g_{h^0\tilde{\chi}_1^0\tilde{\chi}_1^0,\text{tree}} &\simeq \frac{1}{\sqrt{2}} \left[ \left( g\epsilon_2^{(S,A)} - g'\epsilon_1^{(S,A)} \right) (\sin\alpha \pm \cos\alpha) \right] \\ &\simeq \frac{4}{5} (\sin\beta \mp \cos\beta)^2 \frac{gM_W}{M_2}, \end{aligned} \quad (22)$$

where  $g' = g \tan\theta_W$  is the  $U(1)_Y$  gauge coupling, and the upper (lower) signs again hold for the symmetric (anti-symmetric) higgsino; in the second step we have used the ‘‘unification condition’’ (8) as well as the relation  $\alpha \simeq \beta - \frac{\pi}{2}$ , which holds for  $m_A^2 \gg M_Z^2$ . For the quite small value of  $\tan\beta$  used in Fig. 2 this gives a strong cancellation in the coupling of the symmetric higgsino-like state, which is the LSP for  $\mu < 0$ . As a result, the one-loop correction can easily *dominate* over the tree-level contribution (22). This leads to the behaviour shown in Fig. 2, where the coupling changes sign at  $A \simeq -0.8m_{\tilde{q}}$ .

In Figs. 3a-c we show the chargino-LSP mass splitting, the LSP relic density, and the LSP detection rate in a  $^{76}\text{Ge}$  detector as a function of the gaugino fraction of the LSP eigenstate. We have again chosen  $m_{\tilde{q}} = 430$  GeV,  $\tan\beta = 1.5$  and a large value of  $m_A$ . Note that, unlike in Fig. 2, the physical LSP mass has been kept fixed in Figs. 3; the value of 70 GeV chosen here is close to that which maximizes the estimate of the relic density. Since  $m_{\tilde{\chi}_1^0}$  is kept fixed, both  $M_2$  and the tree-level parameter  $\mu$  ( $|\mu|$ ) vary along the curves; e.g.,  $M_2$  lies between about 150 GeV and 1 TeV, with larger values of  $M_2$  corresponding to smaller gaugino fractions, see eqs.(7a,b). In order to maximize the loop effects we have also varied the  $A$ -parameter slightly. In the region of relatively small  $M_2$ , i.e. large gaugino fraction, the light chargino is somewhat heavier, as shown in Fig. 3a; this reduces the absolute size of the  $\tilde{t} - \tilde{\chi}^\pm$  loop contributions to the  $b \rightarrow s\gamma$  decay amplitude for fixed  $A$ , which in turn allows us to go to slightly larger values of  $|A|$  without violating the bounds (21).

We show three curves in each of Figs. 3. The dotted curves labelled ‘‘no loops’’ have been obtained by switching off the loop corrections discussed in Sec. 2. However, we keep quark-squark loop contributions to the mass matrix of the scalar Higgs bosons [33, 28], as well as  $\tilde{q}$  loop contributions to the  $h^0 gg$  coupling and  $q - \tilde{q}$  loop contributions (box diagrams) to the LSP-gluon coupling [34, 11]. These corrections depend only weakly on the sign of  $A$ , however. On the other hand, the signs of the corrections discussed in Sec. 2 are essentially fixed by the sign of  $A$ , as shown in Fig. 2. In Figs. 3 we therefore show results both for positive (solid) and negative (dashed)  $A$ , keeping  $|A|$  fixed. Since we chose parameters close to those that maximize these loop corrections, the band between the solid and dashed curves in Figs. 3a,b

roughly indicates the range that can be covered by changing the parameters of the squark mass matrix, for fixed values of the parameters appearing in the tree-level chargino and neutralino mass matrices.

The results of Fig. 3a show that loop corrections can change the chargino–LSP mass splitting by about three to four GeV in either direction, as already indicated in Fig. 2. Note that the absolute size of this correction is almost independent of the gaugino fraction. This can be understood from eq.(10b), which shows that the tree-level and loop-induced contributions to  $\Delta m_{\tilde{\chi}}$  are independent of each other as long as the LSP is a higgsino-like state.

The results of Fig. 3b show that in the region of high higgsino purity the relatively modest loop corrections to  $\Delta m_{\tilde{\chi}}$  can change the estimate of the LSP relic density by more than a factor of five. The reason is that here the relic density is essentially determined by co-annihilation processes [6], which depend *exponentially* on the mass splitting [7]. Our calculation includes  $\tilde{\chi}_1^0 \tilde{\chi}_1^\pm$  co-annihilation into  $f\bar{f}'$  and  $W\gamma$  final states through  $W$  exchange, and  $\tilde{\chi}_1^0 \tilde{\chi}_2^0$  co-annihilation into  $f\bar{f}$  final states through  $Z$  exchange, where  $f$  stands for any SM fermion other than the top quark. As is usually done, we show results for the LSP mass density in units of the critical or closure density,  $\Omega_{\tilde{\chi}} \equiv \rho_{\tilde{\chi}_1^0} / \rho_c$ , multiplied with the square of  $h$ , the Hubble constant in units of 100 km/(sec·Mpc); a conservative range for  $h$  is  $0.4 \leq h \leq 0.9$ , with recent measurements clustering around 0.5 – 0.6. One needs  $\Omega_{\tilde{\chi}} h^2 \geq 0.02 - 0.03$  if the LSP is to form the bulk of the galactic Dark Matter haloes, and  $\Omega_{\tilde{\chi}} h^2 \geq 0.15$  if the LSP is to form *all* CDM in models [36] with mixed hot and cold Dark Matter. The results of Fig. 3b show that, if  $A$  is large and positive, a 99.9% pure higgsino state can form galactic haloes, and a 99.5% pure higgsino might form all CDM. On the other hand, if  $A$  is large and negative, one will need at least 1% gaugino fraction, corresponding to  $\epsilon_{1,2} \sim 0.1$ , even for the LSP to be able to form galactic haloes.

Note that the curves in Fig. 3b cross over in the region where the gaugino fraction exceeds several percent. Here the mass splitting between the higgsino-like states becomes so large that the relic density is again determined by the usual  $\tilde{\chi}_1^0 \tilde{\chi}_1^0$  annihilation processes, which in our case mostly proceed through virtual  $Z$  exchange. We saw in Fig. 2 that the loop corrections increase (reduce) the  $Z \tilde{\chi}_1^0 \tilde{\chi}_1^0$  coupling if  $A$  is positive (negative). As a result, the curve for  $A > 0$  reaches its maximum already at a rather small gaugino fraction; in this case the LSP can form all CDM if  $180 \text{ GeV} \leq M_2 \leq 340 \text{ GeV}$ . In contrast, the curve for  $A < 0$  reaches its maximum at larger gaugino fraction; here the LSP can form all CDM only if  $M_2$  falls in the narrow window between 160 and 195 GeV.

In Fig. 3c we show estimates for the LSP detection rate in  $^{76}\text{Ge}$ , ignoring possible energy thresholds and assuming a fixed local LSP mass density. In this case the loop corrections discussed in Sec. 2 can increase the tree-level result by more than two orders of magnitude! This is largely due to the small tree-level value of  $g_{h\tilde{\chi}_1^0\tilde{\chi}_1^0}$  for the given case of a symmetric higgsino-like state, see eq.(22). The turn-over in the region of sizable gaugino fraction is caused by mixing with the bino-like neutralino; note that near the end of the curves shown in Figs. 3,  $M_1$  and  $|\mu|$  are already quite close to each other, so the expression (7a) for  $\epsilon_1$  is no longer reliable.

We emphasize that in this case the band between the solid and dashed curves is *not* a good estimate of the variation of the expected counting rate when the parameters of the stop mass matrix are varied, since for large  $|A|$  the loop corrections dominate over the tree-level contribution to  $g_{h\tilde{\chi}_1^0\tilde{\chi}_1^0}$ , as shown in Fig. 2. The total scattering rate can be made to vanish *exactly* for moderately negative values of  $A$ ; this is related to the change of sign of  $g_{h\tilde{\chi}_1^0\tilde{\chi}_1^0}$  observed in Fig. 2. Note that the scattering rate can vanish even for quite moderate values of

all sparticle masses. This illustrates that it is impossible to give a strict lower bound on the expected LSP detection rate even within the MSSM. Of course, there is no a priori reason for such a cancellation between tree-level and one-loop contributions to occur; indeed, over most of the parameter space the loop corrections *increase* the expected event rate. However, even the most optimistic estimate in Fig. 3c is still several orders of magnitude below the sensitivity of present experiments [37].

Recall that we do not rescale [38] the event rate in regions of parameter space leading to a very small LSP relic density; had we done so, most of the curve for  $A < 0$  would have been below the one for positive  $A$ , as can be seen from Fig. 3b. Finally, we saw in Fig. 2 that for fixed  $|A|$ , the absolute size of  $g_{h\tilde{\chi}_1^0\tilde{\chi}_1^0}$  is somewhat smaller for  $A < 0$  than for  $A > 0$ . We nevertheless find a slightly larger scattering rate for  $A < 0$ , partly because this also gives a slightly smaller value for  $m_{h^0}$ ; the  $h^0$  exchange contribution to the LSP–nucleon scattering matrix element scales like  $g_{h\tilde{\chi}_1^0\tilde{\chi}_1^0}/m_{h^0}^2$ . Destructive interference with various squark loop diagrams [11] also plays a role here.

In Figs. 4a–c we show results similar to those of Figs. 3, but for positive sign of the higgsino mass parameter  $\mu$ . The choices for the other parameters are very similar to those in Figs. 3, except that  $A$  is now fixed along each curve. For this rather small value of  $\tan\beta$ , flipping the sign of  $\mu$  has quite dramatic effects, as already anticipated in our discussion in Sec. 2. In particular the gaugino fraction of the LSP for fixed values of  $M_2$  and  $|\mu|$  has become much larger. Conversely, one has to go to much higher  $M_2$  in order to achieve a given level of higgsino purity; in Figs. 4,  $M_2$  varies between about 0.3 and 1.3 TeV. This also implies that for given higgsino purity the chargino–LSP mass splitting is smaller for  $\mu > 0$  than for  $\mu < 0$ , see eq.(10b). On the other hand, Fig. 4a shows that the size of the loop contributions to this mass splitting is essentially independent of the sign of  $\mu$ , as long as the gaugino fraction is small. Note that for positive  $\mu$ ,  $\Delta m_{\tilde{\chi}}$  can be below 10 GeV for a gaugino fraction as large as 12.5% ( $\epsilon_{1,2} \sim 0.3$ ); this will have ramifications for chargino searches at LEP [9].

The smaller  $\Delta m_{\tilde{\chi}}$  for fixed gaugino fraction also implies a greatly reduced relic density, due to enhanced co-annihilation rates. This is illustrated in Fig. 4b. The increased importance of co-annihilation also helps to explain why the curves in this figure do not cross, in contrast to those in Fig. 3b. Another reason is that in the region of sizable gaugino fraction,  $\epsilon_3$  is smaller for positive  $\mu$ ; this is due to non-leading,  $\mathcal{O}(M_1^{-2})$  terms not included in eq.(7c), which become quite important when the gaugino fraction exceeds several percent. Indeed, for the largest gaugino fractions shown in Figs. 4, our treatment of the loop corrections to the couplings of the LSP may no longer be entirely reliable, as discussed in Sec. 2; however, as anticipated in the same discussion, the relative importance of the loop effects decreases with increasing gaugino fraction.

This is also true for the estimated LSP detection rate shown in Fig. 4c. For the smaller gaugino fractions shown in this figure, we find that the loop corrections can change the estimate by a factor of about two in either direction, whereas for large gaugino fraction the loop effects amount to at most 30%. We note again that, had we re-scaled the event rate for scenarios with small LSP relic density, the loop effects would have been even more important in the region of high higgsino purity. Finally, note that in the region where the gaugino fraction exceeds 5% the counting rate in Fig. 4c exceeds that in Fig. 3c by almost an order of magnitude. This is due to the much larger tree-level value of  $g_{h\tilde{\chi}_1^0\tilde{\chi}_1^0}$  for the anti-symmetric higgsino-like state, see eq.(22). Since now the tree-level value exceeds the loop corrections, we find smaller (larger) counting rates for negative (positive) values of  $A$ .

As a final illustration of the effects of the loop corrections to the masses and couplings of

higgsino-like states, we show in Figs. 5a–c the “geography” of the well-known  $(M_2, \mu)$  plane in the region  $M_2 \gg |\mu|$ ,  $\mu < 0$ . In Fig. 5a these loops have been switched off, while in Figs. 5b,c they have been included with  $A = -2.5m_{\tilde{q}}$  and  $A = +2.5m_{\tilde{q}}$ , respectively. In each case the region to the right of the solid line is excluded by the LEP chargino search limit (20). The long and short dashed curves are contours of constant LSP relic density  $\Omega_{\tilde{\chi}} h^2 = 0.025$  and 0.1, respectively. The remaining lines are contours of constant LSP detection rate in a  $^{76}\text{Ge}$  detector, measured in events/(kg·day); as before, we have assumed a fixed local LSP density when calculating the counting rate.

We see that, depending on the sign of  $A$ , loop corrections to the chargino and neutralino mass matrices can significantly reduce (Fig. 5b) or increase (5c) the size of the region that is excluded by chargino searches at LEP; this is a direct result of the change in  $\Delta m_{\tilde{\chi}}$  depicted in Fig. 3a. Similarly, the loop corrections can increase or decrease the region where the LSP is a good CDM candidate; recall that  $\Omega_{\tilde{\chi}} h^2 \geq 0.025$  is required if LSPs are to form the bulk of galactic Dark Matter haloes. Finally, we again observe a dramatic change of the expected LSP detection rate due to radiative corrections. Note that this rate changes only very slowly in Figs. 5b,c, whereas at tree-level one expects a significant dependence on  $M_2$ , see Fig. 5a.

We note in passing that results similar to those displayed in Figs. 3 and 5 can also be obtained in the framework of a recently proposed [39] model with non-unified gaugino masses and a higgsino-like LSP. This model attempts a supersymmetric interpretation of an event with an  $e^+e^-$  pair, two hard photons, and missing transverse momentum  $p_T$  reported by the CDF collaboration [40]. The prospects for detecting relic neutralinos in this model have recently been studied in refs.[41], using tree-level results for the neutralino mass matrix and LSP couplings. We expect that loop corrections of the type discussed here can modify these estimates significantly. However, searches for additional events with two hard photons and missing  $p_T$  failed to find additional candidates [42], casting doubt on any supersymmetric interpretation of the single anomalous event. We therefore do not study this model in any further detail.

## 4.) Summary and Conclusions

In this paper we have presented a calculation of loop corrections involving Yukawa couplings to the masses and couplings of the higgsino-like states of the MSSM. We have found these corrections to be very sensitive to the size and sign of the soft supersymmetry breaking  $A$  parameters. If  $|A|$  is large, the one-loop prediction for the difference of the chargino and LSP masses can differ by up to  $\sim \pm 4$  GeV from the tree-level estimate; the loop correction to the  $\tilde{\chi}_2^0 - \tilde{\chi}_1^0$  mass difference is about twice as big. Combinations of parameters leading to even larger corrections lead to conflicts with the measured value of the branching ratio for inclusive  $b \rightarrow s\gamma$  decays, and/or with the negative outcome of searches for Higgs bosons at LEP. We also found that for negative sign of the higgsino mass parameter  $\mu$ , one-loop corrections to the LSP coupling to  $Z$  and Higgs bosons can be comparable to or even larger than the tree-level contributions already for quite moderate gaugino masses,  $M_2 \geq 200$  GeV.

We have illustrated the importance of these loop corrections by computing their effect on the estimated LSP relic density and on the direct LSP detection rate, assuming the LSP to be higgsino-like. The relic density is in this case often determined by co-annihilation processes, the rate of which depends exponentially on the mass splittings between the higgsino-like states. Yukawa loop corrections can therefore change the tree-level prediction by a factor of  $\sim 5$  in



either direction. This re-introduces a state with more than 99% higgsino purity as a viable cold Dark Matter candidate, if the corrections to the mass splittings are near the upper end of their allowed range. If  $\mu < 0$ , the effect of loop corrections on the estimated LSP counting rate is even more dramatic: The predicted rate might increase by two orders of magnitude, but it might also be exactly zero (for spinless nuclei), even if all sparticle masses are in or below the few hundred GeV range. Clearly effects of this size have to be included in any quantitative analysis of the properties of higgsino-like Dark Matter.

We conclude with some remarks regarding the viability of models with higgsino-like LSP. Within the framework of minimal supergravity models [43], which assume universal scalar masses as well as unified gaugino masses at the Grand Unification scale, a higgsino-like LSP is possible only if  $\tan^2 \beta \gg 1$ , and if scalar soft breaking masses are significantly larger than gaugino masses. Since gaugino masses in turn must be considerably larger than  $|\mu|$  for the LSP to be higgsino-like, naturalness arguments favour a very light LSP in such a scenario. On the other hand, the parameter space leading to a higgsino-like LSP opens up considerably if one allows the sparticle spectrum at the GUT scale to be non-universal. In particular, the predicted value of  $|\mu|$  can be reduced either by giving larger soft breaking masses to the Higgs bosons than to third generation squarks, or by reducing the gluino mass compared to the masses of the electroweak gauginos. We therefore conclude that a higgsino-like LSP with mass slightly below  $M_W$  can be a viable cold Dark Matter candidate, both from the phenomenological and from the model building point of view.

## Acknowledgements

M.D. thanks the members of the Center for Theoretical Physics at Seoul National University as well as the KEK theory group for their hospitality during the course of this work. M. M. N. was supported in part by the Grant-in-aid for Scientific Research from the Ministry of Education, Science and Culture of Japan(07640428).

## Appendix: Expressions for $C$ -Functions

In Sec. 2 we gave general expressions for the one-loop corrections from Yukawa interactions to the  $Z\tilde{\chi}_1^0\tilde{\chi}_1^0$  vertex, eqs.(12), as well as for the  $\phi\tilde{\chi}_1^0\tilde{\chi}_1^0$  and  $A\tilde{\chi}_1^0\tilde{\chi}_1^0$  couplings, eqs.(16), in terms of the  $C$ -functions defined in ref.[16]. However, as already mentioned in Sec. 2, the expressions for the  $C$ -functions contain apparent divergencies both in the limit  $s \rightarrow 4m_{\tilde{\chi}_1^0}^2$  relevant for the calculation of the LSP relic density, and in the limit  $s \rightarrow 0$  relevant for the calculation of the LSP-nucleon scattering cross section.<sup>¶</sup> In case of the higher  $C$ -functions the necessary cancellations become too delicate for a reliable numerical treatment even if “double precision” variables are used. We have therefore re-evaluated the relevant Feynman parameter integrals in these two kinematical limits, which allows us to express the  $C$ -functions appearing in Sec. 2 as combinations of  $B$ -functions. These expressions are collected in this Appendix.

In our notation the scalar three-point function  $C_0$  is defined as

$$C_0(s, m^2, M_1, M_2, M_3) = - \int_0^1 dy \int_0^y dx \left[ m^2 y^2 + s(x^2 - xy) + y (M_2^2 - M_3^2 - m^2) \right]$$

---

<sup>¶</sup>Recall that eqs.(12) and (16) have been written in a convention where both momenta  $k_1$  and  $k_2$  point towards the vertex. In case of LSP-nucleon scattering the sign of one these momenta therefore has to be inverted.

$$+x(M_1^2 - M_2^2) + M_3^2 - i\epsilon]^{-1}; \quad (\text{A.1})$$

this definition coincides with that used in Appendix C of ref.[16]. This gives:

$$C_0(4m^2, m^2, M_1, M_2, M_3) = \frac{1}{D} \left[ B_0(m^2, M_1, M_3) + B_0(m^2, M_2, M_3) - 2B_0(4m^2, M_1, M_2) \right]; \quad (\text{A.2a})$$

$$C_0(0, m^2, M_1, M_2, M_3) = \frac{1}{M_1^2 - M_2^2} \left[ B_0(m^2, M_1, M_3) - B_0(m^2, M_2, M_3) \right], \quad (\text{A.2b})$$

where

$$D = 2 \left( m^2 + M_3^2 \right) - M_1^2 - M_2^2. \quad (\text{A.3})$$

In the limit  $M_1 \rightarrow M_2$ , eq.(A.2b) reduces to:

$$C_0(0, m^2, M, M, M_3) = -\frac{1}{2m^2} \left[ \log \frac{M^2}{M_3^2} + \frac{M_3^2 + m^2 - M^2}{\sqrt{|\Delta|}} \cdot L \right], \quad (\text{A.4})$$

where we have introduced

$$\Delta = 2m^2 \left( M^2 + M_3^2 \right) - m^4 - \left( M^2 - M_3^2 \right)^2; \quad (\text{A.5a})$$

$$L = \begin{cases} 2 \arctan \frac{\sqrt{\Delta}}{M^2 + M_3^2 - m^2}, & \Delta \geq 0 \\ \log \frac{M^2 + M_3^2 - m^2 + \sqrt{-\Delta}}{M^2 + M_3^2 - m^2 - \sqrt{-\Delta}}, & \Delta < 0 \end{cases}. \quad (\text{A.5b})$$

If eqs.(A.2) are used for  $C_0$ , the function  $C_1^+$  defined in ref.[16] has apparent divergencies only at  $s \rightarrow 4m^2$  (we suppress the imaginary infinitesimal  $-i\epsilon$  from now on):

$$\begin{aligned} C_1^+(4m^2, m^2, M_1, M_2, M_3) &= - \int_0^1 dy \int_0^y dx \frac{y/2}{m^2(y-2x)^2 + y(M_2^2 - M_3^2 - m^2) + x(M_1^2 - M_2^2) + M_3^2} \\ &= \frac{1}{2D} + \frac{1}{D^2} \left\{ M_3^2 \left[ B_0(m^2, M_1, M_3) + B_0(m^2, M_2, M_3) \right] \right. \\ &\quad + m^2 \left[ B_2(m^2, M_3, M_1) + B_2(m^2, M_3, M_2) \right] \\ &\quad + \frac{M_1^2 - M_2^2}{2} \left[ B_1(m^2, M_3, M_1) - B_1(m^2, M_3, M_2) \right] \\ &\quad - \left[ 2 \left( m^2 + M_3^2 \right) + M_2^2 - M_1^2 \right] B_0(4m^2, M_1, M_2) \\ &\quad \left. + 2 \left( M_2^2 - M_1^2 \right) B_1(4m^2, M_2, M_1) + 8m^2 B_3(4m^2, M_1, M_2) \right\}, \quad (\text{A.6}) \end{aligned}$$

where  $D$  has been defined in eq.(A.3). Here we have used the higher  $B$  functions as defined in ref.[44]; recall that our definition of  $B_1$  differs by an overall sign from that of ref.[16].

Similarly, after application of eqs.(A.2), the function  $C_1^-$  contains apparent divergencies only at  $s = 0$ :

$$C_1^-(0, m^2, M_1, M_2, M_3) = - \int_0^1 dy \int_0^y dx \frac{x - y/2}{m^2 y^2 + y(M_2^2 - M_3^2 - m^2) + x(M_1^2 - M_3^2) + M_3^2}$$

$$\begin{aligned}
&= \frac{1}{2(M_1^2 - M_2^2)} \left\{ \left( 1 + 2 \frac{M_2^2 - M_3^2}{M_1^2 - M_2^2} \right) [B_1(m^2, M_3, M_2) - B_1(m^2, M_3, M_1)] \right. \\
&\quad - \frac{2m^2}{M_1^2 - M_2^2} [B_3(m^2, M_3, M_2) - B_3(m^2, M_3, M_1)] \quad (\text{A.7}) \\
&\quad \left. + \frac{2M_3^2}{M_1^2 - M_2^2} [B_0(m^2, M_2, M_3) - B_0(m^2, M_1, M_3)] - 1 \right\}.
\end{aligned}$$

Note that by construction [16],  $C_1^- \rightarrow 0$  as  $M_1 \rightarrow M_2$ .

The functions  $C_2^+$  and  $C_2^-$  only appear in the  $Z$  vertex, eqs.(12). Moreover, the coefficient in front of  $C_2^+$  vanishes for  $s \rightarrow 4m_{\tilde{\chi}_1^0}^2$ , while the coefficient in front of  $C_2^-$  vanishes for  $s \rightarrow 0$ . We therefore only need to consider  $C_2^+$  in the limit  $s \rightarrow 0$ :

$$\begin{aligned}
C_2^+(0, m^2, M_1, M_2, M_3) &= - \int_0^1 dy \int_0^y dx \frac{y^2/4}{m^2 y^2 + y(M_2^2 - M_3^2 - m^2) + x(M_1^2 - M_3^2) + M_3^2} \\
&= \frac{1}{4(M_1^2 - M_2^2)} [B_2(m^2, M_3, M_2) - B_2(m^2, M_3, M_1)]. \quad (\text{A.8})
\end{aligned}$$

In the limit  $M_1 \rightarrow M_2$ , this reduces to

$$C_2^+(0, m^2, M, M, M_3) = \frac{1}{4} [B_1'(m^2, M_3, M) + B_0'(m^2, M_3, M) + C_0(0, m^2, M, M, M_3)], \quad (\text{A.9})$$

where  $C_0(0, m^2, M, M, M_3)$  is given in eq.(A.4), and  $B_0'$  and  $B_1'$  are the derivatives of  $B_0$  and  $B_1$  with respect to their first argument.<sup>||</sup> Similarly, we need  $C_2^-$  only in the limit  $s \rightarrow 4m^2$ :

$$\begin{aligned}
C_2^-(4m^2, m^2, M_1, M_2, M_3) &= - \int_0^1 dy \int_0^y dx \frac{(x - y/2)^2}{m^2(y - 2x)^2 + y(M_2^2 - M_3^2 - m^2) + x(M_1^2 - M_2^2) + M_3^2} \\
&= \frac{1}{4D} [B_2(m^2, M_3, M_1) + B_2(m^2, M_3, M_2) \\
&\quad + 8B_3(4m^2, M_1, M_2) - 2B_0(4m^2, M_1, M_2)], \quad (\text{A.10})
\end{aligned}$$

where  $D$  is again given by eq.(A.3).

Finally, we note that the divergent function  $C_2^0$  that appears in eqs.(12) can be computed from the general expression given in eq.(C4) of ref.[16], using the results for  $C_0$ ,  $C_1^+$  and  $C_1^-$  collected in this Appendix.

## References

- [1] H. Goldberg, Phys. Rev. Lett. **50**, 1419 (1983); J. Ellis, J. Hagelin, D.V. Nanopoulos, K. Olive and M. Srednicki, Nucl. Phys. **B238**, 453 (1984).
- [2] For a review, see G. Jungman, M. Kamionkowski and K. Griest, Phys. Rep. **267**, 195 (1996).

---

<sup>||</sup>Of course, eq.(A.9) can also be written as derivative of  $B_2$  with respect to its *last* argument, since all two- and three-point functions only depend on the squares of the masses appearing as arguments. However, conventionally one only uses derivatives with respect to the first argument.

- [3] P.F. Smith et al., Nucl. Phys. **B206**, 333 (1982).
- [4] L. Roszkowski, Phys. Lett. **B262**, 59 (1991), and **B278**, 147 (1992).
- [5] M. Drees and M.M. Nojiri, Phys. Rev. **D47**, 376 (1993).
- [6] S. Mizuta and M. Yamaguchi, Phys. Lett. **B298**, 120 (1993).
- [7] K. Griest and D. Seckel, Phys. Rev. **D43**, 3191 (1991).
- [8] D. Pierce and A. Papadopoulos, Phys. Rev. **D50**, 565 (1994), and Nucl. Phys. **B430**, 278 (1994); A.B. Lahanas, K. Tamvakis and N.D. Tracas, Phys. Lett. **B324**, 387 (1994).
- [9] G.F. Giudice and A. Pomarol, Phys. Lett. **B372**, 253 (1996).
- [10] C.-H. Chen, M. Drees and J.F. Gunion, Phys. Rev. Lett. **76**, 2002 (1996).
- [11] M. Drees and M.M. Nojiri, Phys. Rev. **D48**, 3483 (1993).
- [12] H.E. Haber and G.L. Kane, Phys. Rep. **117**, 75 (1985).
- [13] J.F. Gunion and H.E. Haber, Nucl. Phys. **B272**, 1 (1986); Nucl. Phys. **B402**, 567 (1993).
- [14] J. Ellis and S. Rudaz, Phys. Lett. **128B**, 248 (1983).
- [15] M. Drees and M.M. Nojiri, Nucl. Phys. **B369**, 54 (1992).
- [16] W. Beenakker, S.C. van der Marck and W. Hollik, Nucl. Phys. **B365**, 24 (1991).
- [17] G.F. Giudice and E. Roulet, Nucl. Phys. **B316**, 429 (1989).
- [18] J. Silk, K. Olive and M. Srednicki, Phys. Rev. Lett. **55**, 257 (1985); M. Kamionkowski, Phys. Rev. **D44**, 3021 (1991); F. Halzen, T. Stelzer and M. Kamionkowski, Phys. Rev. **D45**, 4439 (1992).
- [19] M. Drees and M.M. Nojiri, Phys. Rev. **D49**, 4595 (1994); A. Djouadi and M. Drees, Phys. Rev. **D51**, 4997 (1995).
- [20] K. Griest, M. Kamionkowski and M.S. Turner, Phys. Rev. **D41**, 3565 (1990); K. Olive and M. Srednicki, Phys. Lett. **B230**, 78 (1989); Nucl. Phys. **B355**, 208 (1991); J. MacDonald, K.A. Olive and M. Srednicki, Phys. Lett. **B283**, 80 (1992).
- [21] M. Drees and A. Yamada, Phys. Rev. **D53**, 1586 (1996).
- [22] M.S. Turner, E.I. Gates and G. Gyuk, astro-ph 9601168.
- [23] J.R. Ellis and R.A. Flores, Nucl. Phys. **B307**, 883 (1988).
- [24] V.A. Bednyakov, H.V. Klapdor-Kleingrothaus and S. Kovalenko, Phys. Rev. **D50**, 7128 (1994).
- [25] T. Mori, Talk presented at the 2nd RESCEU International Symposium on *Dark Matter in the Universe and its Direct Detection*, Tokyo, November 26–28, 1996.

- [26] D0 collab., S. Abachi et al., Phys. Rev. Lett. **76**, 2222 (1996).
- [27] Particle Data Group, R.M. Barnett et al., Phys. Rev. **D54**, 1 (1996).
- [28] Y. Okada, M. Yamaguchi and T. Yanagida, Phys. Lett. **B262**, 54 (1991).
- [29] CLEO collab., M.S. Alam et al., Phys. Rev. Lett. **74**, 2885 (1995).
- [30] S. Bertolini, F. Borzumati, A. Masiero and G. Ridolfi, Nucl. Phys. **B353**, 591 (1991).
- [31] A.J. Buras, M. Misiak, M. Münz and S. Pokorski, Nucl. Phys. **B424**, 374 (1994).
- [32] H.A. Baer and M. Brhlik, hep-ph 9610224.
- [33] Y. Okada, M. Yamaguchi and T. Yanagida, Prog. Theor. Phys. **85**, 1 (1991); R. Barbieri, M. Frigeni and F. Caravaglio, Phys. Lett. **B258**, 167 (1991); H.E. Haber and R. Hempfling, Phys. Rev. Lett. **66**, 1815 (1991); J. Ellis, G. Ridolfi and F. Zwirner, Phys. Lett. **B257**, 83 (1991), and **B262**, 477 (1991).
- [34] M. Drees and M.M. Nojiri, Phys. Rev. **D47**, 4226 (1993).
- [35] D.N. Schramm, as in ref.[25].
- [36] For example, J.R. Primack, J. Holtzman, A. Klypin and D.O. Caldwell, Phys. Rev. Lett. **74**, 2160 (1995).
- [37] D.O. Caldwell et al., Phys. Rev. Lett. **61**, 510 (1988); **65**, 1305 (1990); D. Reuner et al., Phys. Lett. **B255**, 143 (1991); J.J. Quenby et al., Phys. Lett. **B351**, 70 (1995).
- [38] T.K. Gaisser, G. Steigman and S. Tilav, Phys. Rev. **D34**, 2206 (1986); A. Bottino, N. Fornengo, G. Mignola and L. Moscoso, Astroparticle Physics **3**, 65 (1995).
- [39] S. Ambrosanio, G.L. Kane, G.D. Kribs, S. Martin and S. Mrenna, Phys. Rev. Lett. **76**, 3498 (1996), and hep-ph 9607414.
- [40] S. Park for the CDF collab., *Search for new phenomena in CDF*, talk presented at the *10th Topical Workshop on Proton Antiproton Collider Physics*, R. Raha and G. Yodh, eds.
- [41] K. Freese and M. Kamionkowski, hep-ph 9609370; A. Bottino, N. Fornengo, G. Mignola, M. Olechowski and S. Scopel, astro-ph 9611030.  
The relic density of this LSP has first been estimated by G.L. Kane and J.D. Wells, Phys. Rev. Lett. **76**, 4458 (1996).
- [42] D. Toback for the CDF collab., talk presented at the conference of the Division of Particles and Fields of the American Physical Society, Minneapolis, MN, August 1996; D0 collab., S. Adachi et al., hep-ex 9612011.
- [43] For a review, see M. Drees and S.P. Martin, hep-ph 9504324, and references therein.
- [44] M. Drees, K. Hagiwara and A. Yamada, Phys. Rev. **D45**, 1725 (1992).

## Figure Captions

**Fig. 2:** The chargino–LSP mass difference (solid), the axial–vector  $Z\tilde{\chi}_1^0\tilde{\chi}_1^0$  coupling (long dashed), and the  $h^0\tilde{\chi}_1^0\tilde{\chi}_1^0$  coupling (short dashed) as a function of the soft breaking  $A$  parameter, including one–loop corrections involving Yukawa couplings. “Low” and “high” leading–order estimates for the branching ratio for inclusive radiative  $b$  decays are also shown; for our assumption of exactly universal weak–scale soft breaking squark masses, this gives the strongest constraints on  $A$  in the region of interest, as discussed in the text. All quantities have been re–scaled, as indicated.

**Fig. 3:** The chargino–LSP mass difference (a), the LSP relic density  $\Omega_{\tilde{\chi}}h^2$  (b), and the expected LSP detection rate in a  $^{76}\text{Ge}$  detector (c), as a function of the gaugino fraction, defined as the sum of the squares of the gaugino components of the LSP eigenvector. These results are for a fixed LSP mass, so that both  $M_2$  and  $\mu$  vary along the text. Further,  $|A|$  has been decreased from  $2.7m_{\tilde{q}}$  to  $2.5m_{\tilde{q}}$  as  $M_2$  was increased from about 150 GeV to 1 TeV.

**Fig. 4:** As in Fig. 3, but for positive sign of  $\mu$ ; also,  $|A|$  has been kept fixed in this figure, and  $m_{\tilde{\chi}_1^0}$  has been reduced by 2 GeV, in order to be closer to the region of parameter space where the prediction for  $\Omega_{\tilde{\chi}}h^2$  is maximized.

**Fig. 5:** In the region of the  $(\mu < 0, M_2)$  half–plane corresponding to a higgsino–like LSP, we show contours of constant  $\Omega_{\tilde{\chi}}h^2$  (dashed) and contours of constant LSP detection rate (CR) in a  $^{76}\text{Ge}$  detector, in units of events/(Kg · day) (dotted and dot–dashed); note that the values on the latter contours are different for Figs. (a) (no Yukawa loop corrections), (b) ( $A < 0$ ) and (c) ( $A > 0$ ). The region to the right of the solid line is excluded by our interpretation of the LEP chargino search limit, as discussed in the text.